Supporting Information

Extending Rigid Electron-Deficient Skeleton and Appending Electron-Rich Unit to Build High-efficiency Red-Emitting Pyrene-derived TADF Materials

Xiang Chang,[#a] Kaiyu Lu,[#a] Kai Jiang,[a] Bin Ma,[a] Jingwei Huang,[a, b] Xiangqin Gan,[a] Yu Liu,[a, c] Junting Yu[a, c*], and Weiguo Zhu[a*]

[a] School of Materials Science and Engineering, Jiangsu Engineering Laboratory of Light-Electricity-Heat Energy-Converting Materials and Applications, Jiangsu Key Laboratories of Environment-Friendly Polymers, National Experimental Demonstration Center for Materials Science and Engineering, Changzhou University, Changzhou 213164, P. R. China.

[b] State Key Laboratory of Coordination Chemistry, Jiangsu Key Laboratory of Advanced Organic Materials, School of Chemistry and Chemical Engineering, Nanjing University, Nanjing, 210023 P. R. China

[c] Kunshan Bye Polymer Material Corporation, LTD, Suzhou, 215300, P. R. China

Email addresses: zhuwg18@126.com (W. G. Zhu)

Table of Contents

1. Experimental section

1.1 Materials and methods

All reagents and chemicals were purchased from commercial sources and used directly without any further purification unless stated otherwise. Column chromatography was carried out with Merck silica gel (200 ~ 300 mesh). Thin-layer chromatography (TLC) with Merck pre-coated was adopted to monitor reactions until the reactants were consumed completely. All reactions were performed under a nitrogen atmosphere to avoid the oxidation of the reactants by oxygen.

^{1}H-NMR and ^{13}C-NMR spectra were recorded at room temperature on Bruker Avance III NMR spectrometer and the chemical shifts (δ) are reported in parts per million (ppm) using tetramethyl silane (TMS) signals as internal standards. Matrix-assisted laser desorption ionization time of flight mass spectrometry (MALDI- TOF-MS) was performed with Bruker Daltonics AutoflexTM III using α-cyano- 4-hydroxycinnamic acid (CCA) as matrix. Elemental analysis was measured with Vario EL III elementary analyzer. Cyclic voltammetry (CV) was performed using CHI630E at a scan rate of 100 mV s^{-1}. All experiments were carried out in a three-electrode compartment cell with a Pt-wire counter electrode, a Pt-disk working electrode and Ag/AgCl reference electrode. The supporting electrolyte used was 0.1 M tetrabutylammonium hexafluorophosphate ($^{n}Bu_4NPF_6$) solution in dry acetonitrile under a nitrogen atmosphere using ferrocene (Fc) as the calibrant. The (HOMO)and (LUMO) levels are calculated by assuming the energy level of ferrocene/ferrocenium to be -4.8 eV. The thermal gravimetric analysis (TGA) was performed on a TA Instruments (TGA 50) under nitrogen gas flow with a heating rate of 20 ^{o}C min^{-1}. Ultraviolet-visible (UV-Vis) absorption spectra were carried out on Shimadzu UV-2600 spectrometer. The photoluminescence (PL) spectra were recorded on Edinburgh FLS1000, while time-resolved measurements were carried out using time-correlated single-photon counting (TCSPC) spectrometer (Edinburgh FLS1000), and EPL 450 laser were used as excitation source, and delayed life VPL450 laser in the Edinburgh Transient Fluorescence Spectrometer. Low temperature phosphorescence spectra were

performed in film at 77 K on Edinburgh FLS1000 Spectrometer. The photo-luminescence quantum yields (PLQYs) were recorded with an integrating sphere coupled with Edinburgh FLS1000 under ambient condition.

Quantum chemical calculations were performed with Gaussian 09 program, in which density functional theory (DFT) and time-dependent DFT (TD-DFT) calculations were performed at the B3LYP/6-31g (d) level. The optimal geometries, as well as the highest occupied molecular orbital (HOMO) and the lowest unoccupied molecular orbital (LUMO) for both emitters were obtained by DFT calculations. The excited states (S_n and T_n states) and NTOs (natural transition orbitals) were obtained by TD-DFT calculations.

1.2 Preparation of OLEDs

The prepatterned ITO substrates were cleaned with isopropyl alcohol, acetone, detergent and deionized water in an ultrasonic bath. Afterwards, the substrates were dried in the oven at 80 °C. After UV-ozone treatment for 15 min, the PEDOT:PSS layer was directly spin-coated on the ITO substrate as the hole-injecting layer, and then the substrate was transferred into the glovebox filled with N_2 and annealed at 150 °C for 15 min. Then, PVK was spin-coated as hole-transporting layer and annealed at 120 °C for 15 min. The emissive layer was also prepared by spin-coating directly on the hole-transporting layer. Finally, DPEPO as the hole-blocking material, TmPyPB as the electron-transporting material, LiF as the electron- injecting material and aluminum as the cathode material were consecutively thermally evaporated onto the emissive layer in a vacuum chamber of 1×10^{-4} Pa.

1.3 Measurements of EL properties

The EL spectra and current density (*J*)-voltage (*V*)-Radiance (*R*) curves are obtained using a PHOTO RESEARCH Spectra Scan PR 735 photometer and a KEITHLEY 2400 Source Meter constant current source at room temperature. The EQE values are done from the luminance, current density, and EL spectrum on the premise of a Lambertian distribution.

1.4 Synthesis

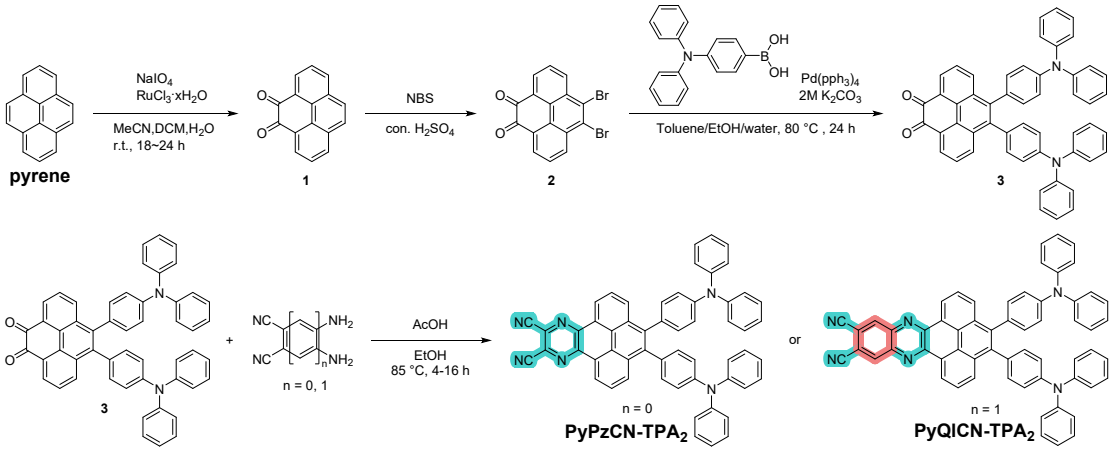

Scheme S1. Synthetic routes for **PyPzCN-TPA$_2$** and **PyQlCN-TPA$_2$.**

Pyrene-4,5-dione (1)

In a round bottom flask, pyrene (10.00 g, 49.50 mmol, 1.0 eq.) and $RuCl_3 \cdot xH_2O$ (1.23 g, 4.74 mmol, 0.096 eq.) were dissolved in 200 mL of acetonitrile. $NaIO_4$ (42.75 g, 198 mmol, 4.0 eq.) was dissolved in 100 mL of hot water and carefully added to the pyrene solution. Another 100 mL of DCM was added and the reaction mixture was vigorously stirred for 18 h at room temperature. After filtration of the suspension through Celite, the filtrate was extracted with DCM (3×100 mL) and the combined organic phases were washed with saturated aqueous $Na_2S_2O_3$ and water and then dried over Na_2SO_4. After removing the solvent under reduced pressure. The crude product was obtained as a dark-orange solid (7.56 g, 66 %). The crude product was purified by column chromatography on silica gel. 3.25 g red bright-orange pyrene-4,5-dione (**1**) crystal was obtained. Yield 27 %.

^{1}H NMR (300 MHz, Chloroform-*d*): δ/ppm, 8.42 (dd, J = 7.4, 1.3 Hz, 2H), 8.12 (dd, J = 8.0, 1.3 Hz, 2H), 7.79 (s, 2H), 7.71 (t, J = 7.7 Hz, 2H). ^{13}C NMR (75 MHz, Chloroform-*d*): δ/ppm, 135.75, 132.00, 130.08, 128.33, 127.98, 127.26. MODI-TOF - MS: m/z calculated for $C_{16}H_8O_2$ $[M]^+$: 232.05; found: 232.09. Elemental analysis (%) for $C_{16}H_8O_2$: C 82.75, H 3.47, O 13.78; found: C 82.73, H 3.48, O 13.47.

9,10-dibromopyrene-4,5-dione (2)

In a round bottom flask, to a solution of pyrene-4,5-dione (**1**) (2.00 g, 8.62 mmol 1.0 eq.) in 20 ml concentrated sulfuric acid. N-bromosuccinimide (2.75 g, 15.50 mmol, 1.8 eq.) was added at 0 °C and stirred for 15 minutes. Then stirred for 1 hour at room temperature. The reaction mixture was precipitated in 2 L water/ice, collected by filtration, washed with water and methanol. Then dried under high vacuum to give 9,10-dibromopyrene-4,5-dione (**2**) in quantitative yield as bright yellow solid.

^{1}H NMR (500 MHz, DMSO-d_6, 120 °C): δ/ppm, 8.72 (d, J = 8.3 Hz, 2H), 8.47 (d, J = 7.4 Hz, 2H), 7.98 (t, J = 7.9 Hz, 2H). Mp: 360 °C (decomposition). Elemental analysis (%) calculated $C_{16}H_6Br_2O_2$: C 49.27, H 1.55, Br 40.97, O 8.20; Found: C 49.41, H 1.73, Br 41.03, O 8.21.

9,10-bis(4-(diphenylamino)phenyl)pyrene-4,5-dione (3)

The mixture of 9,10-dibromopyrene-4,5-dione (**2**) (2.00 g, 5.16 mmol, 1.0 eq.) and (4-(diphenylamino)phenyl)boronic acid (3.73 g, 12.90 mmol, 2.5 eq.), $Pd(PPh_3)_4$ (486 mg, 0.42 mmol, 0.08 eq.), 2M K_2CO_3 aqueous solution with about 21 mL (5.71 g, 41.28 mmol, 8 eq.) and 21 mL ethanol were dissolved in toluene (75 mL). The solution was heated at 90 ℃ for 24 hours under argon atmosphere. After cooling to room temperature, the mixture was extracted with dichloromethane, and further purified by column chromatography of silica gel using dichloromethane/petroleum as the eluent to give a brown powder of 9,10-bis(4-(diphenylamino)phenyl)pyrene-4,5-dione (**3**) with 1.73 g. Yield: 46 %.

^{1}H NMR (400 MHz, Chloroform-*d*): δ/ppm, 8.51–8.29 (m, 3H), 8.10 (dd, J = 10.8, 8.2 Hz, 2H), 7.81–7.61 (m, 3H), 7.40 (d, J = 8.4 Hz, 1H), 7.35–7.26 (m, 6H), 7.23 (t, J = 6.6 Hz, 4H), 7.16–6.98 (m, 13H).^{13}C NMR (100 MHz, Chloroform-*d*): δ/ppm, 180.55, 180.31, 147.92, 147.66, 147.53, 146.82, 139.47, 138.05, 135.82, 135.36, 134.50, 132.49, 132.30, 132.02, 131.87, 131.81, 131.55, 130.73, 130.27, 130.08, 129.92, 129.87, 129.76, 129.47, 129.41, 128.94, 128.17, 128.11, 127.89, 127.83, 127.34, 124.86, 124.47, 123.43, 123.08, 122.93, 122.80. MODI-TOF-MS: m/z calculated for $C_{52}H_{34}N_2O_2$ $[M]^+$: 718.26; found: 718.27. Elemental analysis (%) for

$C_{52}H_{34}N_2O_2$: C 86.88, H 4.77, N 3.90, O 4.45; found: C 86.90, H 4.75, N 3.88, O 4.47.

4,5-bis(4-(diphenylamino)phenyl)phenanthro[4,5-fgh]quinoxaline-10,11-dicarbonitrile (PyPzCN-TPA$_2$)

In a round bottom flask, 9,10-bis(4-(diphenylamino)phenyl)pyrene-4,5-dione (**3**) (0.50 g 0.70 mmol, 1 eq.), 2,3-diaminomaleonitrile (114 mg, 1.05 mmol, 1.5 eq.) were added into the solution with 20 mL of glacial acetic acid and 20 mL ethanol. And the reaction suspension was reflux overnight under a nitrogen condition. After the reaction complete, the reaction mixture was cooled to room temperature and pour into water. Solid was filtered off, washed with water and dried under vacuum. The crude product was purified by column chromatography on silica gel (eluent: PE/DCM). 0.35 g dark brown powder of **PyPzCN-TPA$_2$** was obtained. Yield 63 %.

^{1}H NMR (500 MHz, Chloroform-*d*): δ/ppm, 9.28 (d, *J* = 17.3 Hz, 2H), 8.36 (dd, *J* = 16.5, 8.0 Hz, 2H), 8.14 – 8.03 (m, 4H), 7.54 (d, *J* = 8.5 Hz, 2H), 7.37 – 7.33 (m, 4H), 7.31 – 7.27 (m, 8H), 7.25 (s, 2H), 7.16 (d, *J* = 7.4 Hz, 4H), 7.11 (d, *J* = 5.1 Hz, 4H), 7.05 (s, 2H).^{13}C NMR (125 MHz, Chloroform-*d*): δ/ppm, 147.96, 147.69, 147.57, 146.83, 143.53, 143.41, 143.30, 139.65, 138.20, 132.79, 132.33, 131.95, 131.70, 131.37, 131.19, 131.04, 130.75, 130.28, 130.23, 129.46, 129.40, 127.76, 127.58, 127.45, 127.32, 126.38, 126.14, 126.02, 125.94, 125.71, 125.12, 124.94, 124.86, 124.70, 124.44, 123.39, 123.06, 123.03, 122.95, 113.76. MODI-TOF-MS: m/z calculated for $C_{56}H_{34}N_6$ $[M]^+$: 790.28; found: 790.30. Elemental analysis (%) for $C_{56}H_{34}N_6$: C 85.04, H 4.33, N 10.63; found: C 85.06, H 4.31, N 10.59.

4,5-bis(4-(diphenylamino)phenyl)phenanthro[4,5-abc]phenazine-11,12-dicarbonitrile (PyQlCN-TPA$_2$)

This compound was synthesized in similar manner to **PyPzCN-TPA**. Using 9,10-bis(4-(diphenylamino)phenyl)pyrene-4,5-dione (**3**) (0.50 g 0.70 mmol, 1 eq.), 4,5-diaminophthalonitrile (166 mg, 1.05 mmol, 1.5 eq.). 0.33 g dark maroon power of **PyQlCN-TPA$_2$** was obtained. Yield 56 %.

^{1}H NMR (400 MHz, Chloroform-*d*) δ/ppm: 9.38 (dd, *J* = 28.8, 7.8 Hz, 2H), 8.55 – 8.51 (m, 2H), 8.30 (t, *J* = 8.4 Hz, 2H), 8.08 – 7.99 (m, 4H), 7.56 (d, *J* = 8.3 Hz, 2H),

7.33 (dt, *J* = 23.9, 7.8 Hz, 12H), 7.16 – 7.05 (m, 12H).^{13}C NMR (100 MHz, Chloroform-*d*): δ/ppm = 147.74, 147.61, 146.71, 146.40, 146.17, 141.99, 141.85, 138.06, 136.96, 136.88, 133.12, 132.68, 132.03, 131.82, 131.38, 131.25, 131.14, 130.83, 130.21, 129.45, 129.39, 128.01, 127.64, 127.59, 127.51, 127.24, 127.11, 126.15, 125.38, 125.20, 124.96, 124.83, 124.41, 123.33, 123.08, 122.97, 115.13, 113.01. MODI-TOF-MS: m/z calculated for $C_{60}H_{36}N_6$ $[M]^+$: 840.30; found: 840.43. Elemental analysis (%) for $C_{60}H_{36}N_6$: C 85.69, H 4.31, N 9.99; found: C 85.70, H 4.32, N 9.97.

2. Supplementary Schemes, Figures and Tables

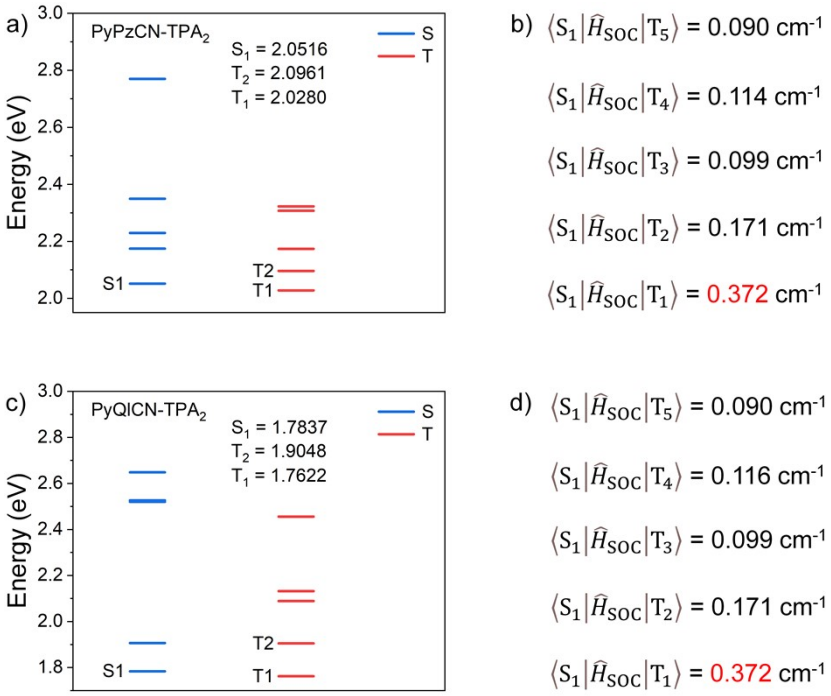

Fig. S1 Adiabatic excitation energies for S_1 and T_n ($n \geq 1$) states, and associated SOC matrix elements ($\langle S_1 | \hat{H}_{soc} | T_n \rangle$) for a), b) **PyPzCN-TPA$_2$** and c), b) **PyQlCN-TPA$_2$** by TD-DFT at the hybrid functional B3LYP-D3/6-31g (d) (H, C, N, O) levels.

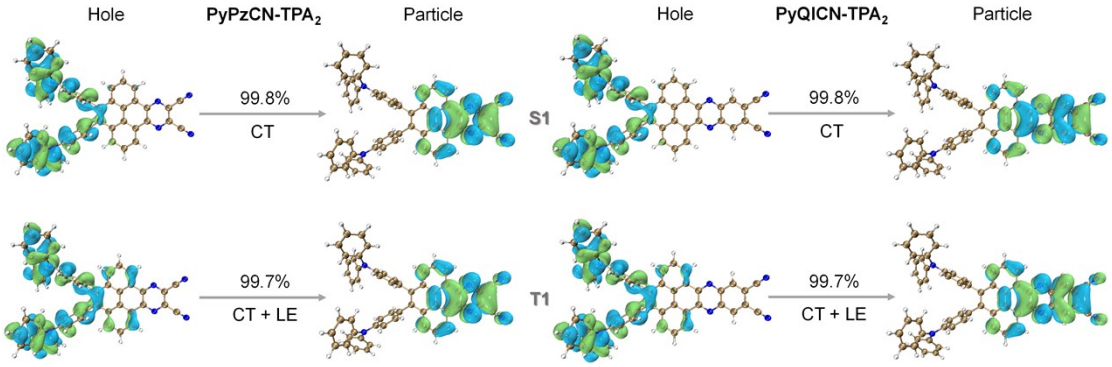

Fig. S2 NTOs of **PyPzCN-TPA$_2$** and **PyQlCN-TPA$_2$** at S_1 and T_2 states.

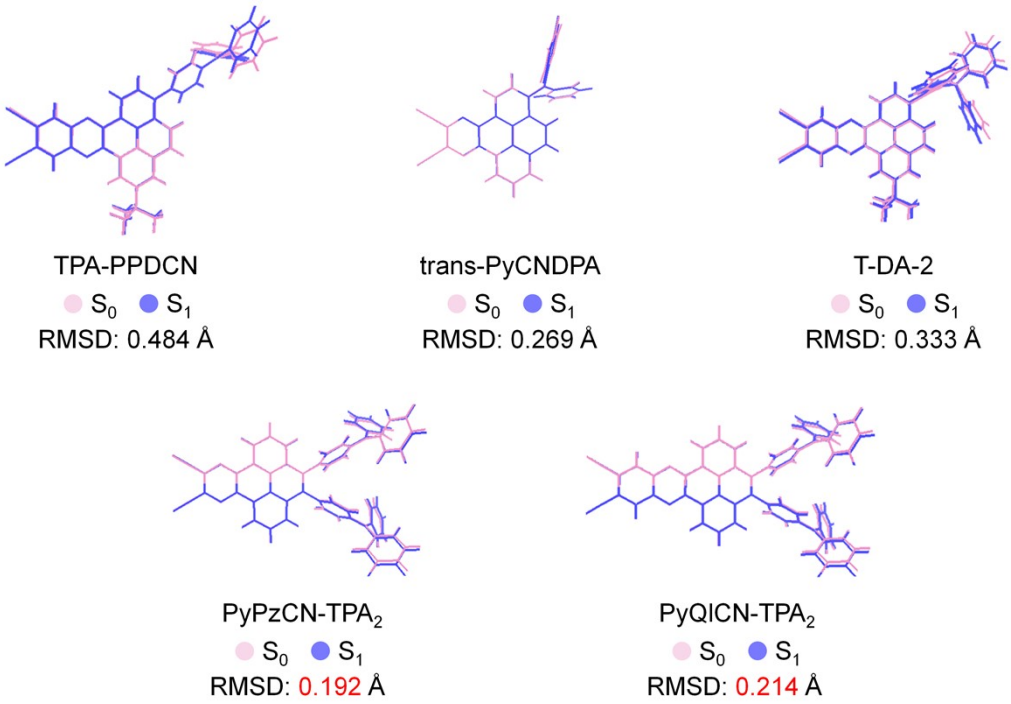

Fig. S3 RMSD of the ground and excited states.

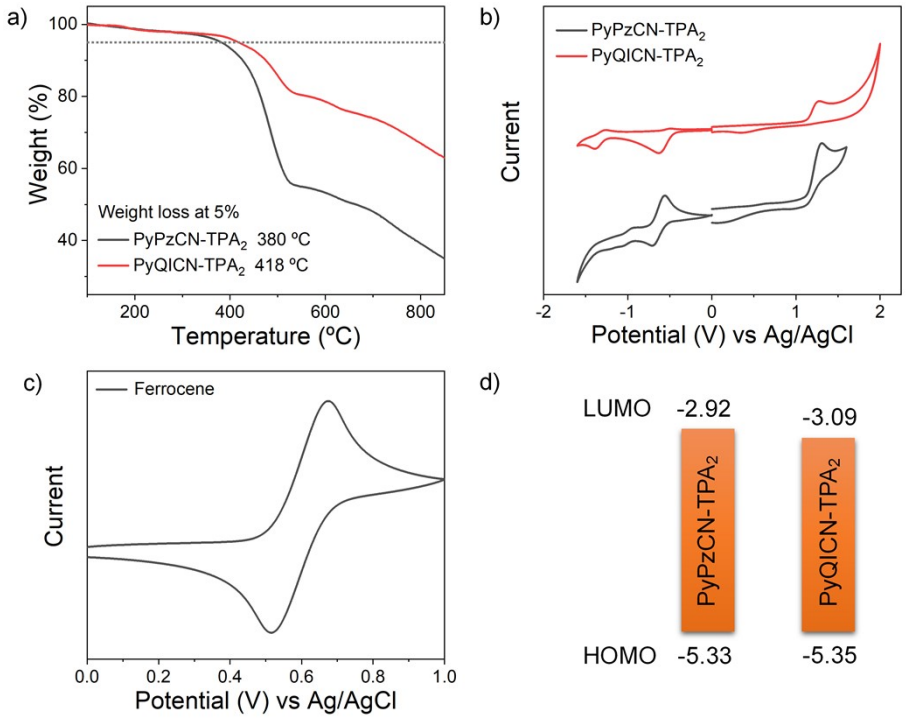

Fig. S4 a) TGA curves of studied **PyPzCN-TPA$_2$** and **PyQlCN-TPA$_2$** under N_2 flow. Cyclic voltammogram curves of b) **PyPzCN-TPA$_2$** and **PyQlCN-TPA$_2$** measured in mixed solution of DCM and CH_3CN (v/v= 1/1) containing 0.1 M tetra-n-butylammonium hexafluorophosphate, c) ferrocene in DCM and CH_3CN mixed solution (v/v=1/1) and d) energy levels.

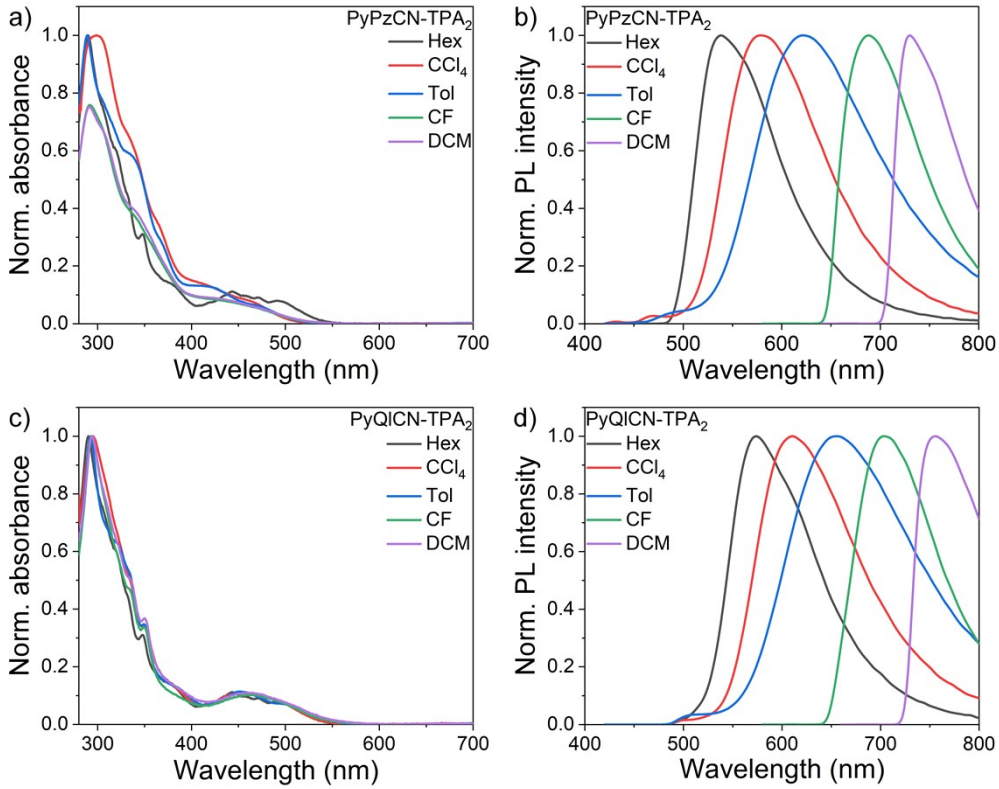

Fig. S5 Normalized absorption a), c) and emission spectra b), d) of **PyPzCN-TPA$_2$** and **PyQlCN-TPA$_2$** in various solvents with concentrations of 10^{-5} M at RT.

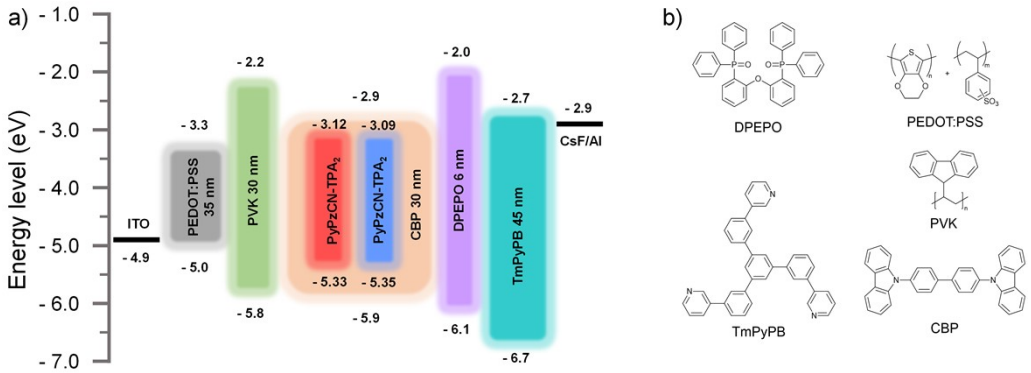

Fig. S6 a) Architectures of the devices and energy diagram, b) molecular structures of the used transport materials.

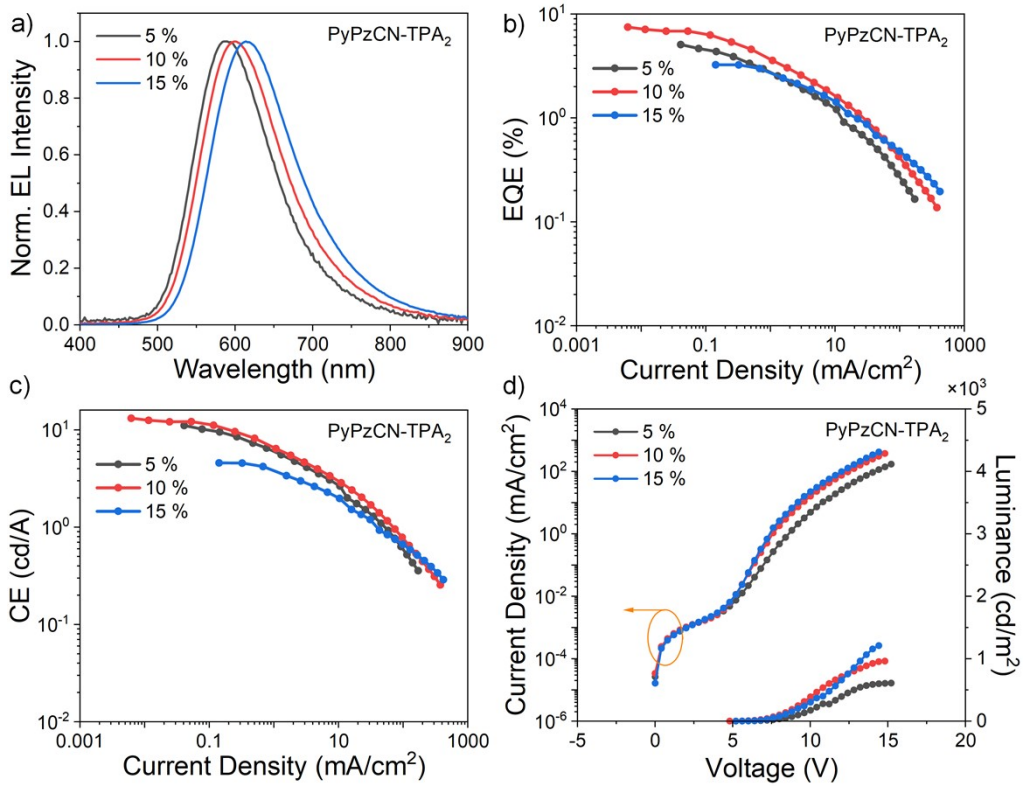

Fig. S7 a) the EL spectra, b) EQE-current density curves, c) current efficiency (CE)-current density curves, d) luminescence and current density versus voltage characteristics of the **PyPzCN-TPA$_2$** with various doping concentrations from 5 % to 15 %.

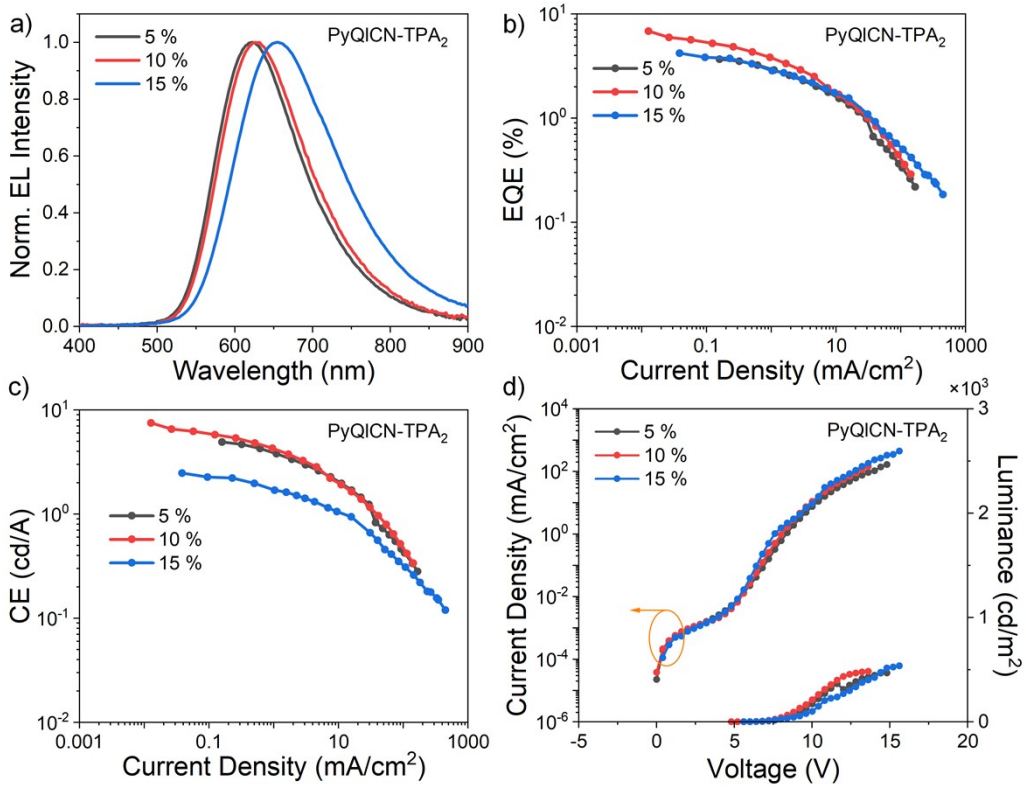

Fig. S8 a) the EL spectra, b) EQE-current density curves, c) current efficiency (CE)-current density curves, d) luminescence and current density versus voltage characteristics of the **PyQlCN-TPA$_2$** with various doping concentrations from 5 % to 15 %.

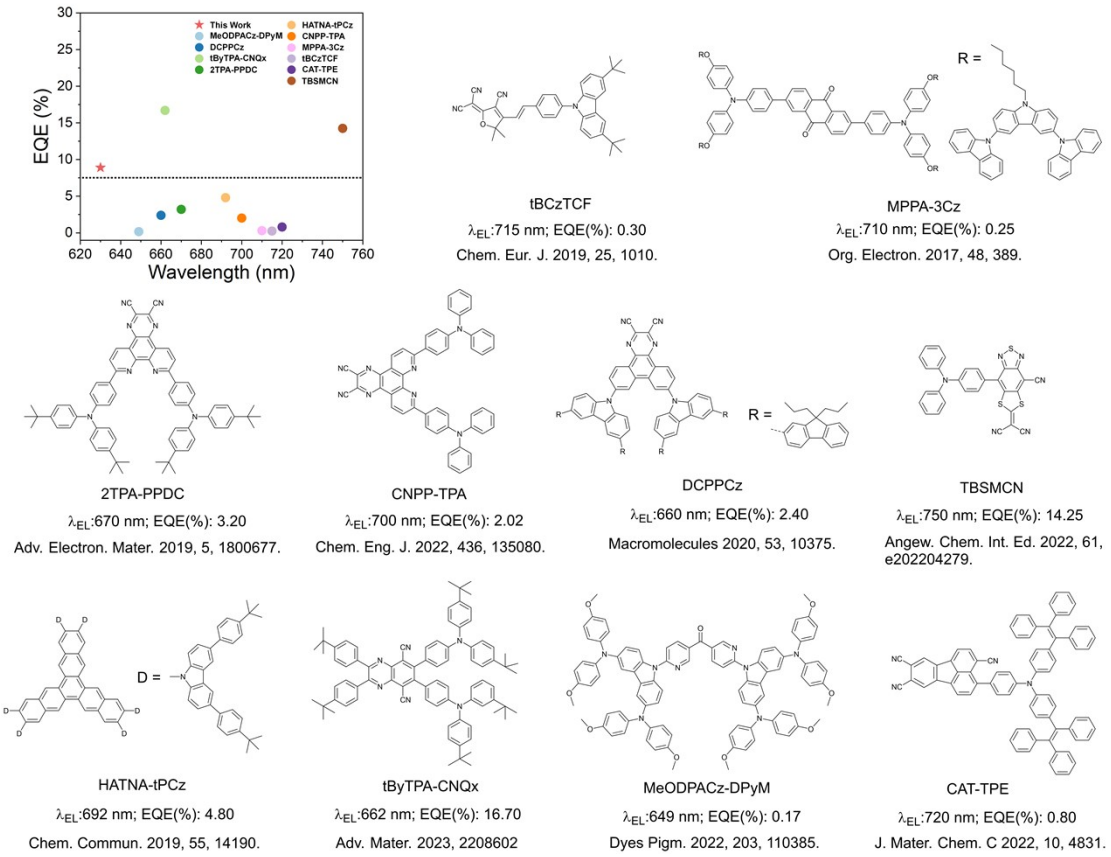

Fig. S9 Summary of EQE versus wavelength plot for the reported red/NIR-emitting TADF materials (620–750 nm) in the solution-processed OLEDs.

Table S1. Contours and energy levels of the first four frontier molecular orbitals of PyPzCN-TPA_2 and PyQlCN-TPA_2 simulated with the TD-DFT method.

Emitter	S_1 (eV)	T_1 (eV)	T_2 (eV)	T_3 (eV)	T_4 (eV)	T_5 (eV)
PyPzCN-TPA_2	2.0516	2.0280	2.0961	2.1739	2.3073	2.3228
PyQlCN-TPA_2	1.7837	1.7622	1.9048	2.0891	2.1319	2.4558

Table S2. Photophysical parameters for the CBP films doped with PyPzCN-TPA$_2$ and PyQlCN-TPA$_2$ at 10 wt% concentration.

Emitter	Φ_p (ns/%)	Φ_d (μs/%)	k_p ($\times10^7$ s^{-1})	k_d ($\times10^4$ s^{-1})	k_{ISC} ($\times10^7$ s^{-1})	k_{RISC} ($\times10^5$ s^{-1})	k_r ($\times10^6$ s^{-1})	k_{nr} ($\times10^4$ s^{-1})
PyPzCN-TPA$_2$	9.42	53.58	4.09	2.57	3.7	1.61	3.85	1.05
PyQICN-TPA$_2$	8.59	56.41	5.15	6.63	4.7	4.77	4.42	2.54

$k_p = 1/\tau_p$ (1)

$k_d = 1/\tau_d$ (2)

$k_{ISC} = (1 - \Phi_p)/k_p$ (3)

$k_{RISC} = k_p k_d \Phi_d / k_{ISC} \Phi_p$ (4)

$k_r = \Phi_p/\tau_p$ (5)

$k_{nr} = 1/\tau_p - k_r$ (6)

$k_{nr} = k_d - k_{ISC}\Phi_p$ (7)

Herein, τ_p and τ_d are the lifetime of prompt and delayed components. Φ_p and Φ_d are the prompt and delayed luminescence quantum efficiency, respectively. The k_p and k_d are the rate constant of prompt and delayed fluorescence. k_{ISC} is the rate constant of intersystem crossing, while k_{RISC} is the rate constant of reverse intersystem crossing between the S_1 and T_1. k_r and k_{nr} are the radiative 1and nonradiative decay rate constant from S_1 to S_0, respectively.

Table S3. Summarized electroluminescent performance of PyPzCN-TPA$_2$ with different doping concentrations.

Dopant	Ratio (wt%)	V_{on} (V)	λ_{EL}[a] (nm)	EQE[b] (%)	L_{max}[c] (cd m^{-2})	CE_{max}[d] (cd A^{-1})	CIE[e] (x, y)
PyPzCN-TPA$_2$	5	5.6	596	5.081	609.7	11.106	0.512,0.468
	10	5.2	600	7.487	961.2	13.168	0.536,0.450
	15	6.0	614	3.245	1210.0	4.582	0.566,0.425

[a]Electroluminescence peaks. [b]Maximum external quantum efficiency. [c]Maximum luminance. [d]Maximum current efficiency. [e]Commission Internationale de L'Eclairage coordinates.

Table S4. Summarized electroluminescent performance of PyQlCN-TPA$_2$ with different doping concentrations.

Dopant	Ratio (wt%)	V_{on} (V)	λ_{EL}[a] (nm)	EQE[b] (%)	L_{max}[c] (cd m^{-2})	CE_{max}[d] (cd A^{-1})	CIE[e] (x, y)
PyQlCN-TPA$_2$	5	6.4	622	3.684	468.2	4.917	0.580,0.406
	10	6.0	626	6.845	483.4	7.497	0.588,0.399
	15	6.4	656	4.202	536.7	2.472	0.613,0.376

[a]Electroluminescence peaks. [b]Maximum external quantum efficiency. [c]Maximum luminance.

[d]Maximum current efficiency. [e]Commission Internationale de L'Eclairage coordinates.

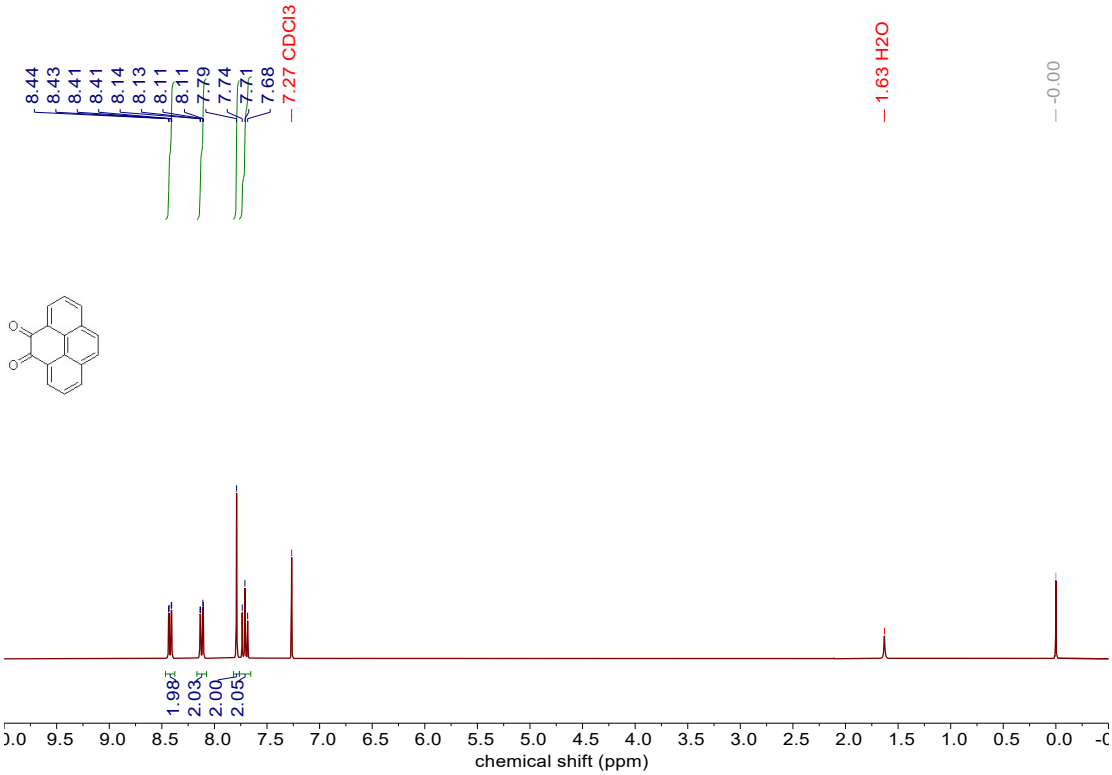

Fig. S10 [1]H NMR spectrum of pyrene-4,5-dione (300 MHz, Chloroform-*d*, 298 K).

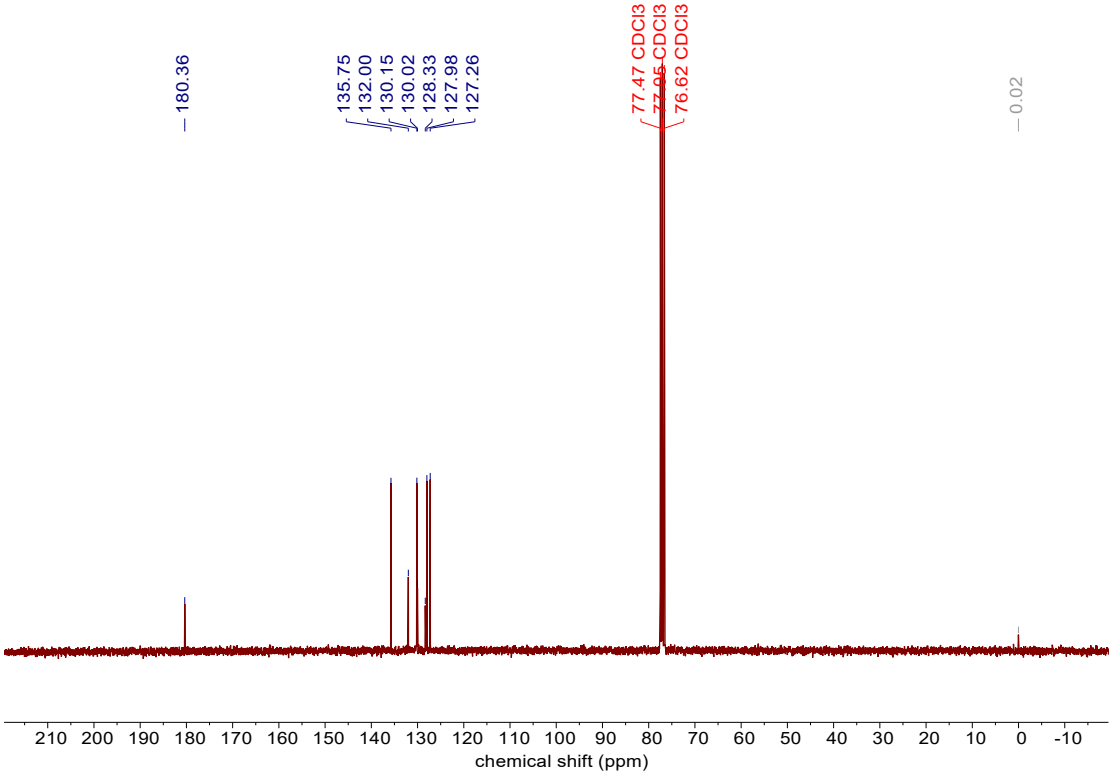

Fig. S11 [13]C NMR spectrum of pyrene-4,5-dione (75 MHz, Chloroform-*d*, 298 K).

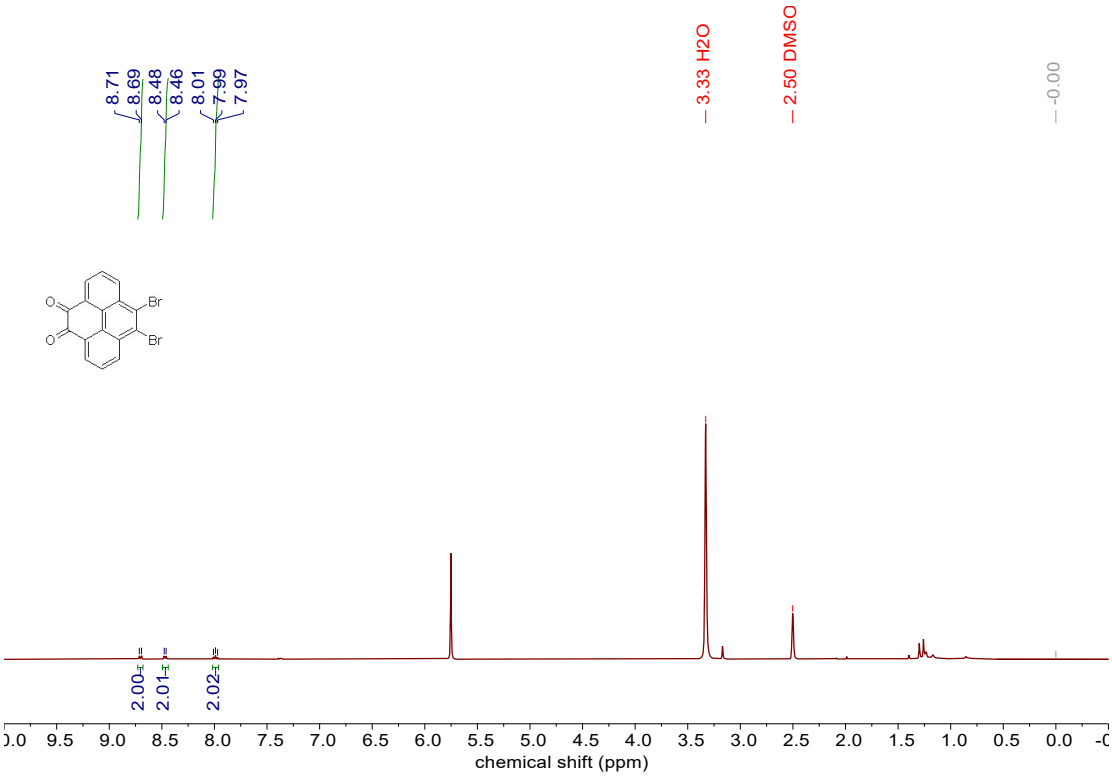

Fig. S12 [1]H NMR spectrum of 9,10-dibromopyrene-4,5-dione (500 MHz, DMSO-d_6, 393 K).

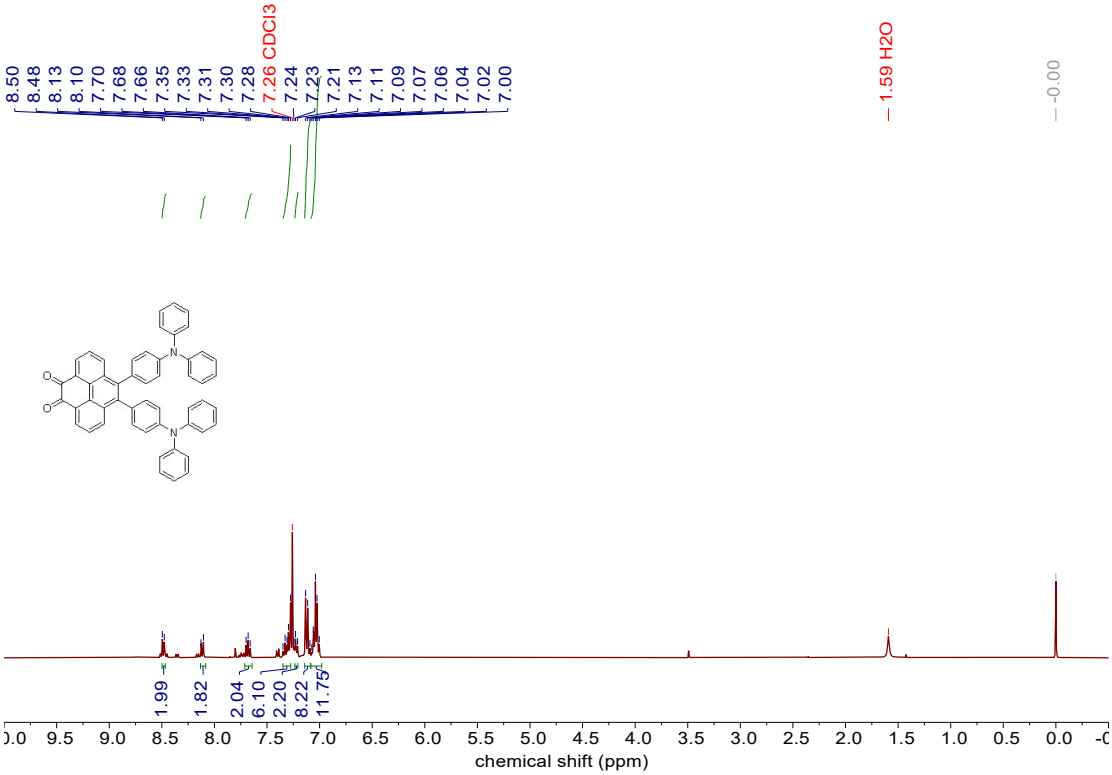

Fig. S13 [1]H NMR spectrum of 9,10-bis(4-(diphenylamino)phenyl)pyrene-4,5-dione (400 MHz, Chloroform-*d*, 298 K).

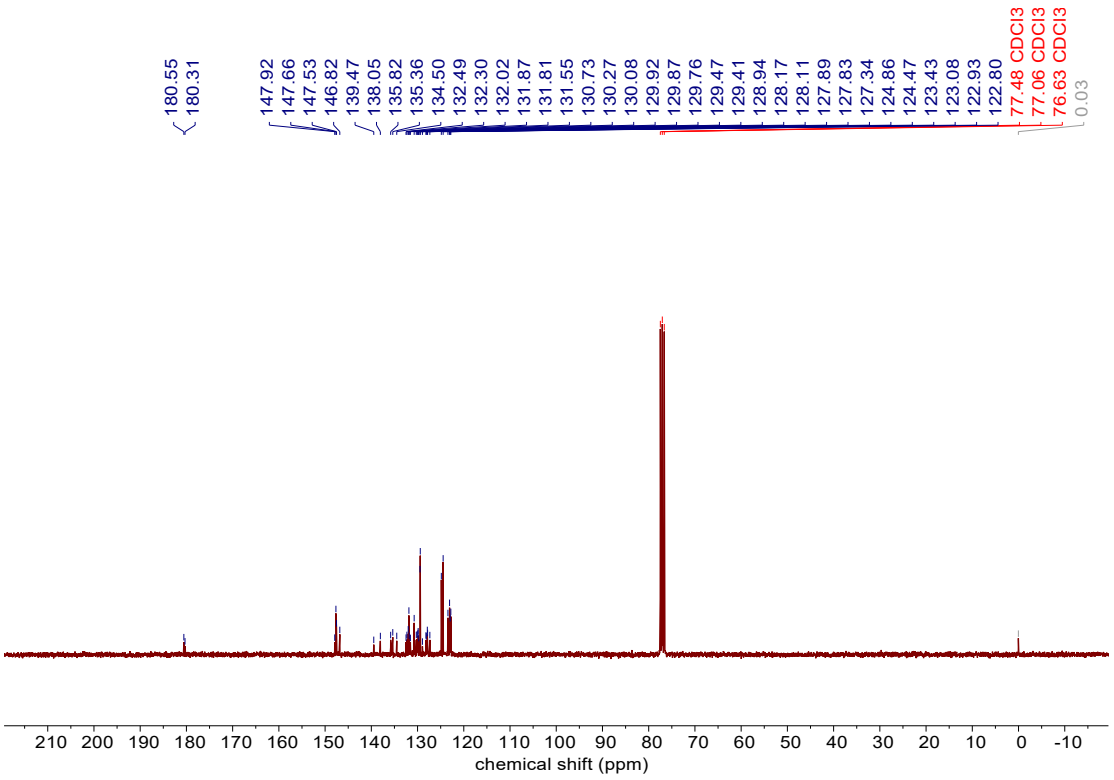

Fig. S14 ^{13}C NMR spectrum of 9,10-bis(4-(diphenylamino)phenyl)pyrene-4,5-dione (75 MHz, Chloroform-*d*, 298 K).

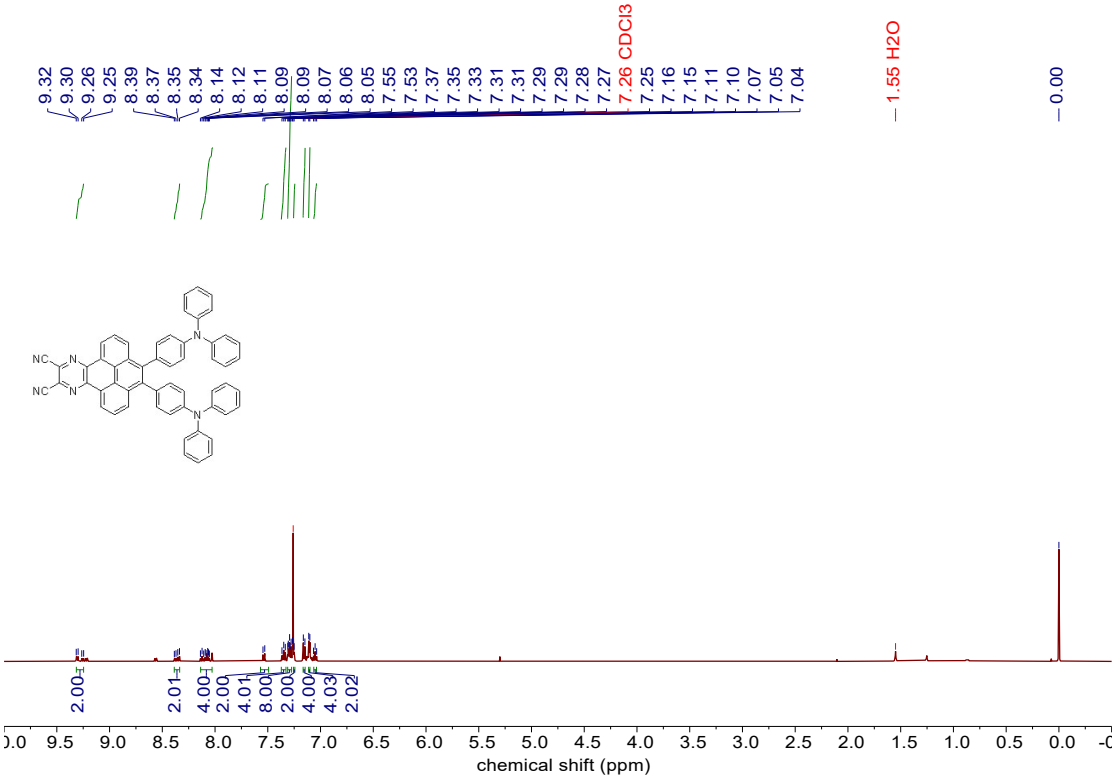

Fig. S15 ^{1}H NMR spectrum of **PyPzCN-TPA$_2$** (400 MHz, Chloroform-*d*, 298 K).

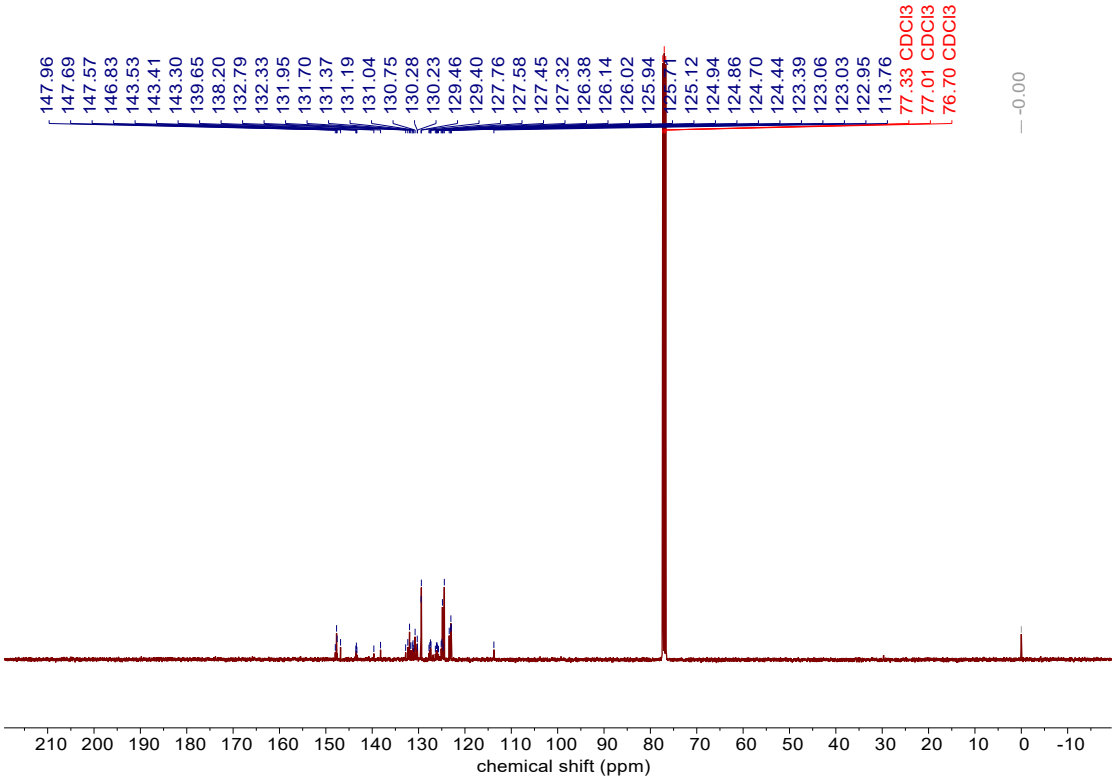

Fig. S16 ^{13}C NMR spectrum of **PyPzCN-TPA$_2$** (101 MHz, Chloroform-*d*, 298 K).

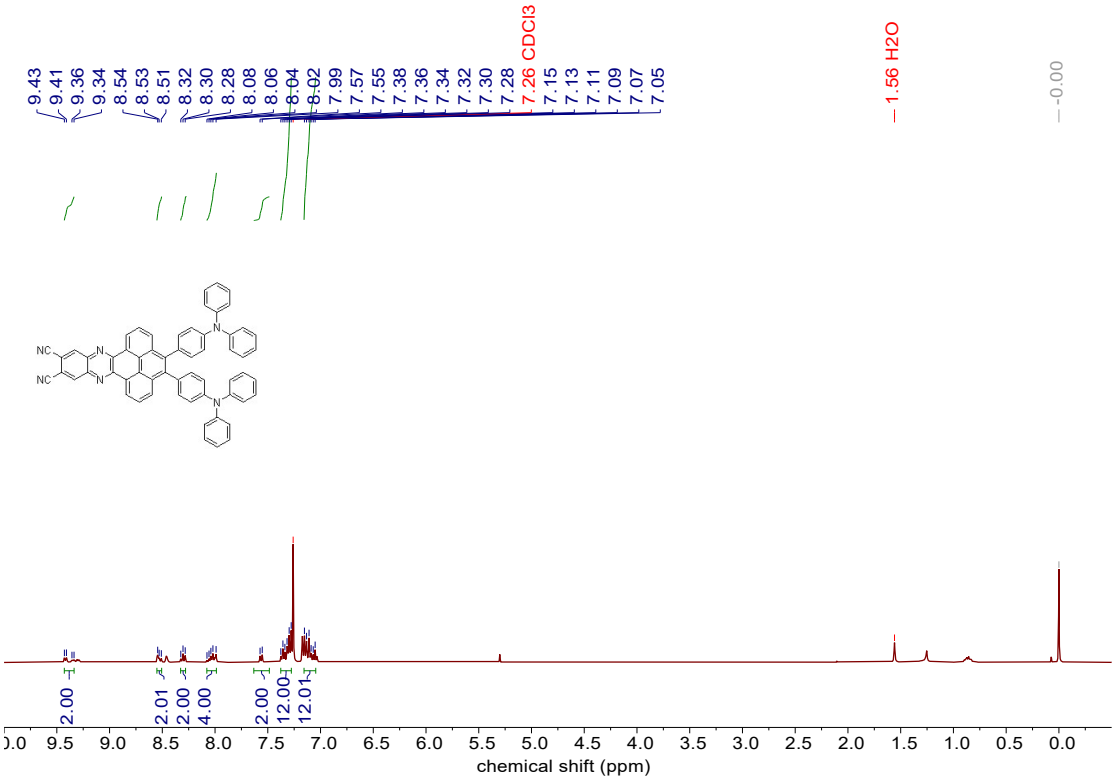

Fig. S17 ^{1}H NMR spectrum of **PyQlCN-TPA$_2$** (400 MHz, Chloroform-*d*, 298 K).

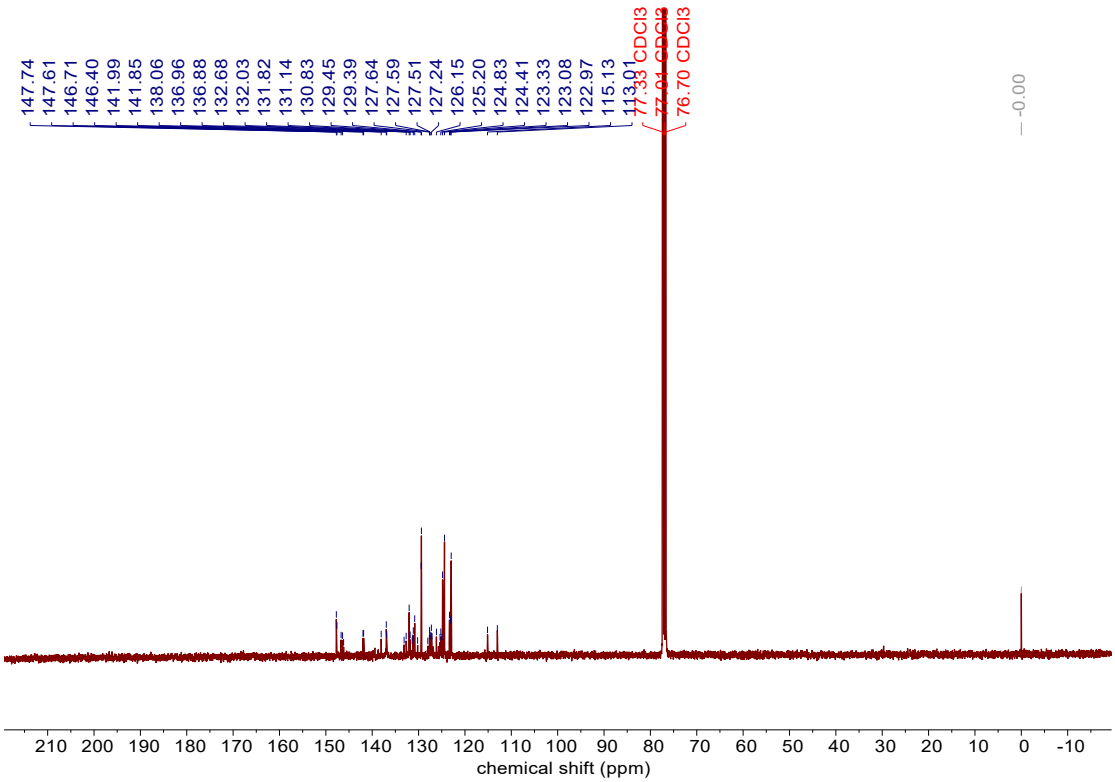

Fig. S18 ^{13}C NMR spectrum of **PyQlCN-TPA$_2$** (101 MHz, Chloroform-*d*, 298 K).

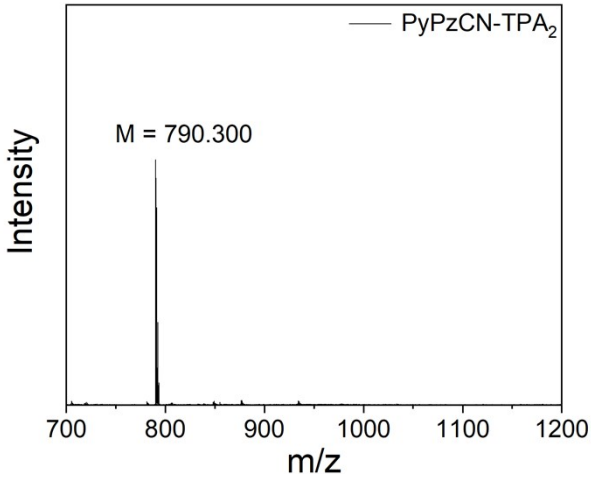

Fig. S19 MALDI-TOF-MS spectrum of **PyPzCN-TPA$_2$**.

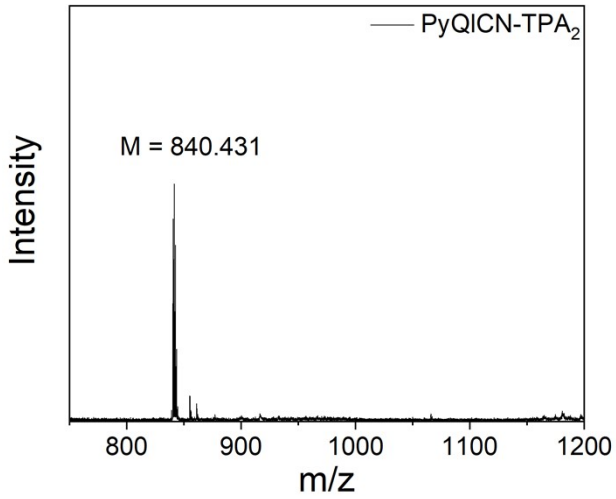

Fig. S20 MALDI-TOF-MS spectrum of **PyQlCN-TPA$_2$**.